PRAMANA
— journal of
physics

Vol. 72, No. 4
April 2009
pp. 727–734

Generation of ultrafast pulse via combined effects of stimulated Raman scattering and non-degenerate two-photon absorption in silicon nanophotonic chip

JIANWEI WU[1,*], FENGGUANG LUO[2,3] and MINGCUI CAO[2,3]
[1]College of Mathematics and Physics, Hohai University, Nanjing 210098, People's Republic of China
[2]College of Optoelectronics Science and Engineering, Huazhong University of Science and Technology, Wuhan 430074, People's Republic of China
[3]Wuhan National Laboratory for Optoelectronics, Wuhan 430074, People's Republic of China
[*]Corresponding author. E-mail: jwwu@hhu.edu.cn

MS received 24 May 2008; revised 8 November 2008; accepted 25 November 2008

Abstract. A project of ultrafast pulse generation has been presented and demonstrated by utilizing the combined nonlinear effects of stimulated Raman scattering (SRS) and non-degenerate two-photon absorption (TPA) based on silicon nanophotonic chip, in which a continuous wave (CW) and an ultrafast dark pulse are co-propagating in the silicon chip so that the CW will be modulated inversely by the dark pulse during the propagation. As a result, an ultrafast bright pulse is achieved using the technique. Simulation results show that an ultrafast pulse with a pulsewidth (full-width at half-maximum (FWHM)) of about 50 fs is generated at the end of a 5-mm long silicon chip, when the initial conditions, including an input maximum of 0.5 W and FWHM of ∼176 fs for dark pulse, and CW with power of 5 W, are chosen.

Keywords. Integrated optics; silicon nanophotonic chip; ultrafast pulse; nonlinear process.

PACS Nos 42.79.Gn; 42.65.Re; 42.65.-k

1. Introduction

Ultrafast pulse sources are of primary importance for applications in such diverse fields as ultrafast optoelectronics and ultrafast spectroscopy. All kinds of schemes have been explored and investigated by researchers so far, in which broad wavelength tunable ultrafast pulse generation is very attractive based on the SRS effect in single mode fibres (SMF) [1,2] and photonic crystal fibres (PCF) [3,4], where long fibre in the range of several metres is required to produce effective Raman gain,

and other affiliated elements are combined for pulse compression and shaping. As a result, it is difficult for optics integration in modern optics communications. Motivated by these limiting factors, we have explored the ultrafast pulse source based on the integrated silicon nanophotonic chip. In fact, over the last few years, as silicon is regarded as a potential integration material, silicon photonics has become a rapidly growing research area, in which many passive and active devices with new or improved functionality have been demonstrated. One important device for optical interconnects is silicon-on-insulator (SOI) ridge waveguide with submicrometer transverse dimensions. Such a SOI device has strong light confinement that can lead to some high nonlinear effects due to high refractive index constant ratio between the silicon core and the silica cladding. In particular, the nonlinear phenomenon from SRS is $\sim 10^4$ times larger compared to the standard single mode glass fibre so that effective Raman gain level can be achieved using silicon waveguides of several millimetres or centimetres. To this day, some significant investigations, such as Raman laser [5], amplification [6], wavelength conversion [7], pulse train generation [8], logic gate [9], filter [10], etc., have been performed based on SOI straight waveguides and ring resonators. In addition, the nonlinear process, such as non-degenerate TPA, will also play an important role for signal propagation, which has already been applied in the all-optical modulation and pulse shaping [11,12]. In this article, another optical function based on these nonlinear effects has been explored and demonstrated in SOI waveguide, where an ultrafast pulse can be generated by the combined effects of SRS and non-degenerate TPA when both the CW and dark pulse are co-propagating along the chip. In fact, a pulse with a pulsewidth of $\sim$20 ps duration has already been achieved based on the modelocking scheme using TPA and free carrier absorption (FCA) induced by TPA processes in silicon waveguide in [13]. Compared to the previous report, the generated ultrafast pulse has the advantage of short duration time and simple operation.

This paper is organized as follows. In §2, the theoretical modelling and equations are presented. In §3, we display the simulation results and discussions. Section 4 summarizes the work.

2. Modelling and equations

In figure 1a, the ridge waveguide structure is with width W, rib height H, and slab height h. Free carriers will be produced when optical waves propagating in SOI waveguide, whose effective recombination lifetime τ_{eff} may be denoted by [14]

$$\tau_{\text{eff}}^{-1} = \frac{S}{H} + \frac{w + 2(H-h)}{wH} S' + 2\frac{h}{H}\sqrt{\frac{D}{w^2}\left(\frac{S+S'}{h}\right)}, \tag{1}$$

where the first term refers to the interface recombination lifetime, the second term refers to the surface recombination at the side walls, and the last term refers to transit time out of the modal area. S and S' are the effective surface recombination velocities and D is the diffusion coefficient.

In figure 1b, the nonlinear interaction between CW and dark pulse will perform in SOI waveguide when they co-propagate, where the wavelengths of CW and dark

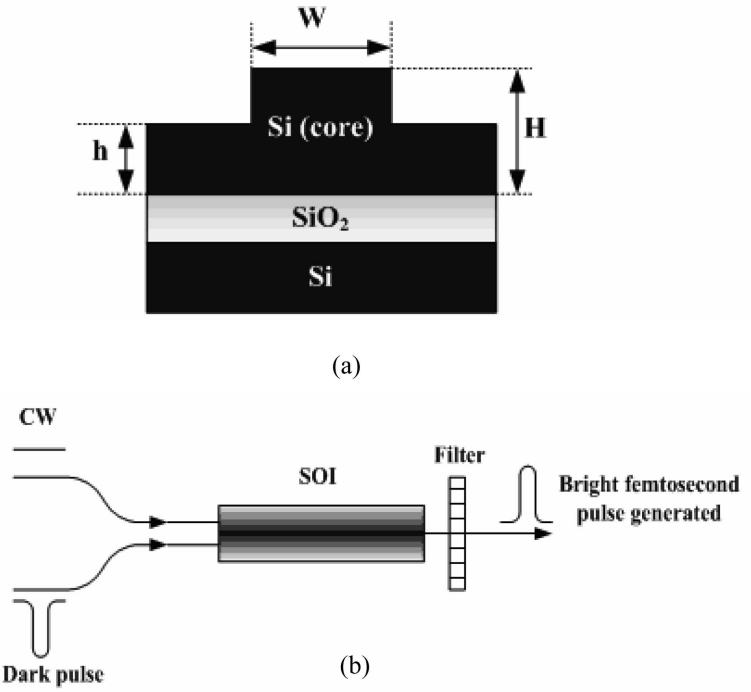

Figure 1. Schematic diagrams of (**a**) cross-section of SOI ridge waveguide and (**b**) the operation principle for the generation of ultrafast pulse.

pulse are set at λ_c and λ_d, respectively. To obtain the effective SRS, the frequency interval should match ∼15.6 THz, i.e., λ_c is set at 1374 nm and λ_d is set at 1480 nm in our investigation. After the CW is modulated by the dark pulse, it will pass through the filter that makes the dark pulse turn off as a result of which the ultrafast pulse is obtained at the end of the device at a wavelength of 1374 nm.

The nonlinear propagation equations modified CW and dark pulse in SOI waveguide can be described by [15,16]

$$\begin{aligned}
&\frac{\partial A_c}{\partial z} + \beta_{c1}\frac{\partial A_c}{\partial t} + i\frac{1}{2}\beta_{c2}\frac{\partial^2 A_c}{\partial t^2} - \frac{1}{6}\beta_{c3}\frac{\partial^3 A_c}{\partial t^3} \\
&= -\frac{1}{2}\alpha_{cl}A_c - \frac{1}{2}\alpha_{cFC}A_c - \frac{1}{2}\frac{\beta_{ccTPA}}{A_{cAeff}}|A_c|^2 A_c \\
&\quad -\frac{\beta_{cdTPA}}{A_{cAeff}}|A_d|^2 A_c + i\gamma_{c,c}|A_c|^2 A_c \\
&\quad +i2\gamma_{c,d}|A_d|^2 A_c + i\frac{2\pi}{\lambda_c}\Delta n_{\lambda c}A_c - \frac{1}{2}g_R\frac{\omega_c}{\omega_d A_{dAeff}}|A_d|^2 A_c, \qquad (2)
\end{aligned}$$

$$\frac{\partial A_d}{\partial z} + \beta_{d1}\frac{\partial A_d}{\partial t} + i\frac{1}{2}\beta_{d2}\frac{\partial^2 A_d}{\partial t^2} - \frac{1}{6}\beta_{d3}\frac{\partial^3 A_d}{\partial t^3}$$

$$= -\frac{1}{2}\alpha_{\mathrm{dl}}A_{\mathrm{d}} - \frac{1}{2}\alpha_{\mathrm{dFC}}A_{\mathrm{d}} - \frac{1}{2}\frac{\beta_{\mathrm{ddTPA}}}{A_{\mathrm{dAeff}}}|A_{\mathrm{d}}|^2A_{\mathrm{d}}$$
$$-\frac{\beta_{\mathrm{dcTPA}}}{A_{\mathrm{dAeff}}}|A_{\mathrm{c}}|^2A_{\mathrm{d}} + i\gamma_{\mathrm{d,d}}|A_{\mathrm{d}}|^2A_{\mathrm{d}}$$
$$+i2\gamma_{\mathrm{d,c}}|A_{\mathrm{c}}|^2A_{\mathrm{d}} + i\frac{2\pi}{\lambda_{\mathrm{d}}}\Delta n_{\lambda\mathrm{d}}A_{\mathrm{d}} + \frac{1}{2}g_{\mathrm{R}}\frac{1}{A_{\mathrm{cAeff}}}|A_{\mathrm{c}}|^2A_{\mathrm{d}}, \tag{3}$$

where the subscript c and d denote CW and dark pulse, respectively, A is the slowly varying pulse envelope, β_1, β_2 and β_3 are the first-, second-, and third-order dispersion coefficients. The parameter β_1 is related to the group velocity ν_{g} of the pulse by $\nu_{\mathrm{g}} = 1/\beta_1$. While β_2 governs the effect of group velocity dispersion (GVD), β_3 governs the effects of third-order dispersion (TOD) and becomes important for ultrashort pulses because of their wide bandwidth. $\gamma = 2\pi n_2/\lambda A_{\mathrm{Aeff}}$ is the nonlinear parameter (n_2 is the nonlinear coefficient, A_{Aeff} is known as the effective core area, λ is the centre wavelength of optical wave), α_{l} is the linear propagation loss. α_{FC} is the FCA coefficient, β_{TPA} is the TPA coefficient, which has identical values for all kinds of TPA processes, g_{R} is the coefficient of Raman gain peak, and ω is the angle frequency. The first four terms on the right-hand side of each equation denote the propagation loss, FCA loss, degenerate TPA and non-degenerate TPA, respectively. The next two terms represent the self-phase modulation and cross-phase modulation, respectively, and the final term describes free carrier dispersion that is related to efficient index change Δn that can be described by

$$\Delta n_{\lambda\mathrm{c,d}} = -8.8\times10^{-22}\cdot\left(\frac{\lambda_{\mathrm{c,d}}}{1.55}\right)^2\Delta n_{\mathrm{e}} - 8.5\times10^{-18}$$
$$\times\left(\frac{\lambda_{\mathrm{c,d}}}{1.55}\right)^2(\Delta n_{\mathrm{h}})^{0.8} \tag{4}$$

and FCA coefficient is written as

$$\alpha_{\mathrm{FC}} = 8.5\times10^{-18}\cdot\left(\frac{\lambda_{\mathrm{c,d}}}{1.55}\right)^2\Delta n_{\mathrm{e}} + 6.0\times10^{-18}\cdot\left(\frac{\lambda_{\mathrm{c,d}}}{1.55}\right)^2\Delta n_{\mathrm{h}}$$
$$= \sigma\cdot n$$
$$= \sigma_0\cdot\left(\frac{\lambda_{\mathrm{c,d}}}{1.55}\right)^2 n, \tag{5}$$

where the coefficient $\sigma_0 = 1.45\times10^{-17}$ cm^2 is the free-carrier absorption cross-section measured at $\lambda = 1.55$ μm. $n = n_{\mathrm{e}} = n_{\mathrm{h}}$ is the density of electron–hole pairs generated by the TPA and non-degenerated TPA processes, and is given by

$$\frac{\mathrm{d}n}{\mathrm{d}T} = -\frac{n}{\tau_{\mathrm{eff}}} + \frac{\beta_{\mathrm{ccTPA}}}{2\hbar\omega_{\mathrm{c}}}(|A_{\mathrm{c}}(z,t)|^2\cdot A_{\mathrm{cAeff}}^{-1})^2$$
$$+\frac{\beta_{\mathrm{ddTPA}}}{2\hbar\omega_{\mathrm{d}}}(|A_{\mathrm{d}}(z,t)|^2\cdot A_{\mathrm{dAeff}}^{-1})^2$$
$$+\frac{\beta_{\mathrm{cdTPA}}}{\hbar\omega_{\mathrm{d}}}(|A_{\mathrm{d}}(z,t)|^2\cdot|A_{\mathrm{c}}(z,t)|^2A_{\mathrm{cAeff}}^{-1})^2$$
$$+\frac{\beta_{\mathrm{dcTPA}}}{\hbar\omega_{\mathrm{c}}}(|A_{\mathrm{c}}(z,t)|^2\cdot|A_{\mathrm{d}}(z,t)|^2A_{\mathrm{dAeff}}^{-1})^2. \tag{6}$$

To observe the characters of ultrafast pulse generated, eqs (1)–(6) can be solved numerically with the determined boundary conditions. In the following section, the detailed simulation investigations will be presented.

3. Numerical simulations and discussions

According to [14,17], the simulation parameters adopted are shown in table 1.

To reduce the influence of dispersion on the dark pulse, the centre wavelength of dark pulse is set at the zero dispersion wavelength, $\lambda_{\mathrm{d}} = 1480$ nm, for the chosen waveguide. In the simulation, the amplitude profile of the initial ultrafast dark pulse can be described by

$$A_{\mathrm{d}}(0,t) = \sqrt{P_{\mathrm{d0}}}\tanh(T/T_{\mathrm{d0}}). \tag{7}$$

In this equation, P_{d0} is the input maximum power and T_{d0} is the pulsewidth. Hence, the corresponding intensity distribution of input dark pulse is shown in figure 2a, where its FWHM is equal to ∼176 fs. At the same time, figures 2b and 2c display the outcome profiles of bright pulse generated and the corresponding phase shift, respectively. In the calculation, the range of time window is from −5 ps to 5 ps, and the initial maximum powers are set at 0.5 W for dark pulse and 5 W

Table 1. Simulation parameters.

Parameter	Definition	Value
n_2	Nonlinear coefficient	6×10^{-18} m$^2 \cdot$ W^{-1}
β_{c1}	The first-order dispersion at CW wavelength	1.351×10^{-8} s $\cdot$ m^{-1}
β_{c2}	The second-order dispersion at CW wavelength	0.2 ps$^2 \cdot$ m^{-1}
β_{c3}	The third-order dispersion at CW wavelength	3.5×10^{-3} ps$^3 \cdot$ m^{-1}
β_{d1}	The first-order dispersion at dark pulse wavelength	1.353×10^{-8} s $\cdot$ m^{-1}
β_{d2}	The second-order dispersion at dark pulse wavelength	0
β_{d3}	The third-order dispersion at dark pulse wavelength	3.8×10^{-3} ps$^3 \cdot$ m^{-1}
g_{R}	Raman gain coefficient	10.5×10^{-9} cm $\cdot$ GW^{-1}
$\alpha_{\mathrm{cl,dl}}$	Waveguide linear loss coefficient	0.22 dB $\cdot$ cm^{-1}
β_{TPA}	Two-photon absorption coefficient	0.5 cm $\cdot$ GW^{-1}
W	Rib waveguide width	900 nm
H	Rib height	780 nm
h	Slab height	390 nm
S, S'	Effective surface recombination velocity	80 m $\cdot$ s^{-1}
D	Diffusion coefficient	16 cm^2 $\cdot$ s^{-1}
h	Reduced Planck constant	1.06×10^{-34} J $\cdot$ s

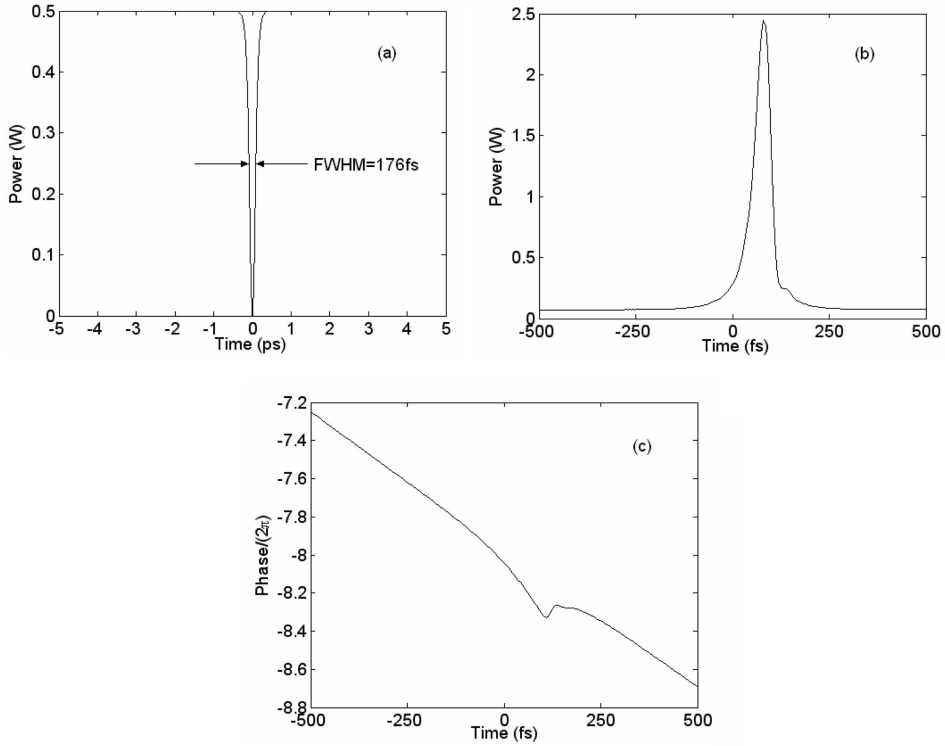

Figure 2. (**a**) The input ultrafast dark pulse, (**b**) the ultrafast pulse generated at the end of 5-mm long waveguide and (**c**) the phase profile of the generated pulse.

for CW. To produce effective Raman resonance between the two optical waves, a CW wavelength of 1374 nm should be chosen, namely, the frequency shift of two wavelengths is equal to ∼15.6 THz that is a prerequisite condition for effective SRS in silicon material. Moreover, the spectrum width of the dark pulse is narrower than the bandwidth of Raman gain so that the Raman gain coefficient for dark pulse can be a constant during SRS. When both dark pulse and CW are co-propagating in silicon waveguide, the energy transfer will occur from the CW to dark pulse, which is proportional to the overlapped energy between the two optical fields. As a consequence, by the nonlinear SRS process, the edges of dark pulse will obtain gain, and the corresponding energy of CW will be quickly depleted. However, the decay of CW energy is very slow between CW and dark pulse. As a result, the CW can be modulated inversely by the dark pulse, namely, an ultrafast pulse may be formed at the output end of the chip, which is plotted in figure 2b, where the obtained bright pulse has only FWHM of about 50 fs. In addition, because the group velocity of dark pulse is small compared to that of CW, the obtained ultrafast pulse will shift backward when compared with the dark pulse in figure 2b, where another noticeable issue is that the trailing edge of the pulse has weak oscillation structure (side lobe) due to the influence of the positive third-order dispersion. In addition, under the

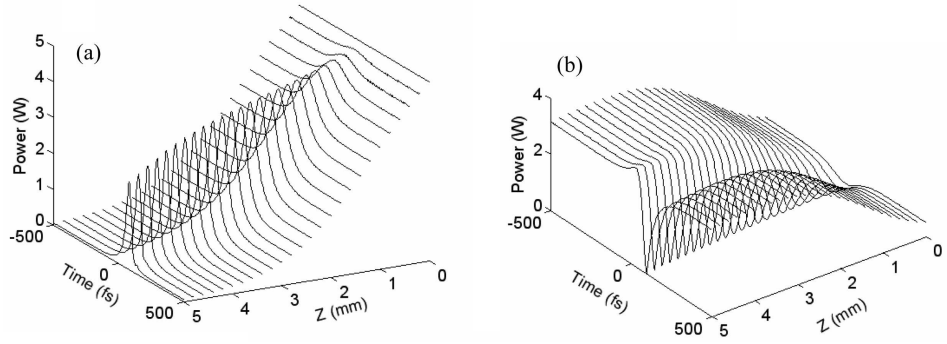

Figure 3. The dynamic evolutions of CW (**a**) and dark pulse (**b**) along the silicon chip.

influences of self-, cross-phase modulations, etc., the phase of the generated pulse will also produce significant change, which is clearly shown in figure 2c. To observe the dynamic evolution of CW and dark pulse along the silicon chip, figures 3a and b illustrate the profiles of optical fields in different chip positions. As can be seen from the figure, the edge of the dark pulse is quickly amplified owing to the strong SRS effect in the initial section of the waveguide. Simultaneously, the corresponding energy of CW is depleted leading to the generation of bright pulse, whereas, the dark pulse which occurs gain saturation because of CW depletion after a propagation distance of about 3-mm long waveguide, i.e., influences of nonlinear losses such as non-degenerate TPA, etc. on the optical fields will overrun the SRS process for further propagation in the chip. From the figure, we can see that when optical waves are propagating from ∼3 mm to ∼5 mm, the pedestal energy of the generated bright pulse is further suppressed, and the corresponding edge energy of the dark pulse is also depleted due to the non-degenerate TPA effect. Therefore, the quality of bright pulse will increase. In addition, it is worth noting that the peak power of the output ultrafast pulse, P_c, is remarkably decayed compared to its launching power mostly due to the linear loss and nonlinear processes that include the TPA, FCA and SRS. In the investigation, the intrapulse Raman scattering is neglected in our investigation, which will only play significant effect for pulsewidth below ∼30 fs [16]. Based on the above analysis, an ultrafast bright pulse can be achieved in silicon nanophotonic chip by adjusting the system parameters such as chip length, and so on.

4. Conclusions

In this paper, we have presented and demonstrated the numerical results of ultrafast pulse generation based on silicon nanophotonic chip with the ridge structure of silicon-on-insulator. Results show that several tens of ultrafast pulse can be achieved by utilizing the nonlinear processes such as stimulated Raman scattering, non-degenerate two-photon absorption, and so on, in silicon waveguide when CW and dark pulse are co-propagating.

Acknowledgements

This work was supported by the Chinese Natural Science Foundation under grant No. 60677023, the Chinese National High Technology Research and Development Program under grant No. 2006AA01Z240, and the Natural Science Foundation of Hohai University under grant No. 2007419011.

References

[1] Y Matsuo, N Nishizawa, M Mori and T Goto, *Opt. Rev.* **7**, 309 (2000)
[2] D B S Soh, J Nilsson and A B Grudinin, *J. Opt. Soc. Am.* **B23**, 1 (2006)
[3] N Nishizawa, Y Ito and T Goto, *Jpn. J. Appl. Phys.* **42**, 449 (2003)
[4] C F Cheng, X F Wang and B F Shen, *Chin. Phys. Lett.* **21**, 1965 (2004)
[5] H S Rong, A S Liu, R Jones, O Cohen, D Hak, R Nicolaescu, A Fang and M Paniccia, *Nature (London)* **433**, 292 (2005)
[6] T K Liang and H K Tsang, *Appl. Phys. Lett.* **85**, 3343 (2004)
[7] Q F Xu, V R Almeida and M Lipson, *Opt. Lett.* **30**, 2733 (2005)
[8] J W Wu and F G Luo, *Prog. Electromagn. Research* **75**, 163 (2007)
[9] C Li, L J Zhou and A W Poon, *Opt. Express* **15**, 5069 (2007)
[10] B D Timotijevie, F Y Gardes, W R Headley, G T Reed, J J Paniccia, O Cohen, D Hak and G Z Masanovic, *J. Opt. A: Pure Appl. Opt.* **8**, S473 (2006)
[11] L Liao, A Liu, D Rubin, J Basak, Y Chetrit, H Nguyen, R Cohen, N Izhaky and M Paniccia, *Electron. Lett.* **43**, 1196 (2007)
[12] I W Hsieh, X G Chen, J I Dadap, N C Panoiu, R M Osgood, S J Mcnab and Y A Ciasov, *Opt. Express* **15**, 1135 (2007)
[13] E K Tien, N S Yuksek, F Qian and O Boyraz, *Opt. Express* **15**, 6500 (2007)
[14] D Dimitropoulos, J R Claps, J C S Woo and B Jalali, *Appl. Phys. Lett.* **86**, 07115 (2005)
[15] V M N Pasaro and F De Leonardis, *Opt. Quantum Electron.* **38**, 877 (2006)
[16] R Dekker, N Usechak, M Forst and A Driessen, *J. Phys. D: Appl. Phys.* **40**, R249 (2007)
[17] Q Lin, J D Zhang, P M Fauchet and G P Agrawal, *Opt. Express* **14**, 4786 (2006)